X-RAY AND GAMMA-RAY COMPUTERIZED MINITOMOGRAPH SCANNER FOR SOIL SCIENCE AND BIOMEDICAL APPLICATIONS

Paulo Estevão Cruvinel, Silvio Crestana, Sergio Mascarenhas
EMBRAPA/UAPDIA, Rua XV de Novembro 1452, 13560 S. Carlos, S.P., Brazil

Roberto Cesareo – Centro per l' Ingegneria Biomedica, Corso Vittorio Emanuele II, 244, 00186, Roma, Italy

ABSTRACT

A X-Ray and Gamma-Ray computerized minitomograph scanner system has been developed for applications in soil science and in biomedical systems. Previous results were obtained using a miniature X-Ray tomograph scanner dedicated to biomedical analysis (Cesareo et al., 1982). As a new methodology in instrumentation and in soil research (Crestana et al., 1986), the minitomograph has proved to be useful for measuring water content ($\theta \pm 3\%$) and soil bulk density ($\rho \pm 1\%$). The system features are : translation and rotation scanning modes, 200 mm effective field of view, oulse counting method for signal processing and 1.0 mm spatial resolution.

The performance of the system was demonstrated by experimentally measuring water content in soil samples collected from the Ap horizon of a Barretos, Brazil, fine sandy loam soil.

Also applications have been carried out of the CT-scanner to biomedical systems, in order to study the absorption of Iodine by plants and Godolinium by internal organs of mice.

1. INTRODUCTION

A new method for investigation in soil science physics has be troduced by Crestana et al. (1985), Hainsworth & Ailmore (198 Petrovic et al. (1982).

This method uses computerized tomography and it has proved to great advantage when compared to the classical methods such a vimetry (Schwab & Frevert, 1985) or gamma-Ray direct transm (Davisson & Evans, 1952).

We have developed a dedicated X-Ray and Gamma-Ray computerize nitomograph scanner for soil science.

The computational programs were all developed in Pascal lan They are used respectively for control and data acquisition, reconstruction and for quantitative analysis of the linear at tion coefficient at any chosen region of the image.

This paper describes the CT-scanner realized in S. Carlos, Brazil and dedicated to soil science. This scanner is very s to the one realized in Rome and employed in many fields, as n structive testing and biomedical applications (Cesareo et al.

2. PRINCIPLES OF THE TOMOGRAPHY METHOD

In tomography a cross-sectional image is obtained by calcul based on profiles of transmitted photon beams along multiple through the body with an adequate algorythm. In the image ob each point represents a linear attenuation coefficient.

Figure 1 schematically shows the situation for discreet scann well as the division in planar section cells (pixels).

The linear attenuation coefficient $\mu(x,y)$ can be calculated the equation

$$N = No \exp\left(-\int_s \mu(x,y)\, ds\right)$$

where N is the number of transmitted photons and No is the number of incident photons along any directions across the sample.

In practice, the integral equation (I-1) becomes a discreet sum. For each profile we have a set of rays-sums resulting in a set of M projections.

In the present work, the images have been reconstructed by using the filtered backprojection algorythm with a Ram-Lack filter (Ramachandran & Lakshminarayanan, 1971).

3. SYSTEM'S DESIGN

The system configuration and block diagram are shown in figure 2 and 3 respectively.

The hardware is basically a mechanical table with two step-motors, one for rotation and another for translation motions; radioactive source: collimators; radiation detector with NaI(T) crystal:electronic pulse counting and processing system; microcomputer with two floppy disk-units 5 1/4"; high resolution video and graphic printer.

We have used an 8 bits microcomputer based on a 65Ø2 microprocessor.

3.1. INTERFACE AND ELECTRONIC PULSE SYSTEM

The interface subsystem has been developed using two peripheral interface adapter 6821 - PIA and 74LSØ4 and CD4Ø5Ø integrated circuits.

We have been using the range of addresses from $CØDØ to $CØDF.

The A ports (PA) of the peripheral interface adapeter A are programmed as output.

These ports are used for step-motors controller. The signals sent through the data register (DRA) are shown in figure 4.

The B ports (PB) of the peripheral interface adapter A have programmed in different modes where PBØ, PB1 are outputs, and PB3, PB4 are inputs.

The PB5, PB6 and PB7 ports are not used. The signals sent a ceived through the data register (DRB) are shown in figure 5.

The signals correspondent to bits Ø and 1 are sent from the computer to the pulse handling system. The test for end cou gnal is sent from the counter to the microcomputer. The A por of the peripheral interface adapter B has been chosen for the acquisition.

The data from the electronic pulse handling system are cod BCD. For the data register (DRA) one will have the configu shown in figure 6.

The B port (PB) of the peripheral interface adapter B is prog to control of the following signals, data transference, digit ce, terminus module (TM) and previous module (PM).

For the data register (DRB) one will have the configuration in figure 7.

The CD4Ø5Ø integrated circuits are used as line buffers im the fan-out and fan-in conditions of the interface and contr cuit. Figure 8 shows the schematic diagram for the interfa control system.

3.2. CONTROL CARDS FOR STEP-MOTORS

This subsystem generate the signals to step-motors. The sign fine the rotating sense, and the control cards leave the pow ge in stand-by when necessary.

Figure 9 illustrates the schematic diagram of one subsystem step-motors' control cards.

3.3. CONTROL CARDS FOR THE TOMOGRAPHIC TABLE POSITION

This subsystem uses optoelectronics devices and comparative circuits to define specific coordinated positions for the tomographic table. The output signals are sent to the PB3 and PB4 ports of the peripheral interface adapter A. Figure 1Ø illustrates a schematic diagram the tomographic table position's control cards.

4. APPLICATIONS TO SOIL SCIENCE

We have applied the computerized minitomograph scanner system to measure water content in soil.

We have used soil samples collected from the Ap horizon of a Barretos, Brazil fine sandy loam soil. Air dried soil was passed through a 1.Ømm sieve and packed into thin wall "plexiglass" boxes. Thickness ranged from 1.9 to 2.1 cm. For packing the soil samples we employed the methodology usually adopted in soil physics (Hillel, 1981).

To obtain samples with different water contents ranging from Ø.8% to 3Ø% we used four samples of soil equilibrated with water. This was obtained adding a known volume of water to a known volume of previously air dried soil.

A typical tomography of a soil sample with 10% water is shown in figure 11; tomographs of soil samples containing various water contents have been also analyzed and the attenuation coefficients have been deduced (figure 12) from the images. Further, the quality of the images has been evaluated by using the plexiglass test object shown in figure 13 (top) and the method of the contrast transfer function (CTF) (Taylor & Lupton, 1986).

Figure 13 (bottom) shows the image of the test object by using a collimation, and a pixel width of 1 mm. Other images have been carried out with collimators of 0.5 and 2 mm diameter.

A loss of spatial resolution at a pixel width of 2 mm can be ed from the images and was confirmed by the CTF, as shown in 14. On the other hand, the spatial resolution was not impro decreasing the pixel width to 0.5 mm.

5. APPLICATIONS TO BIOMEDICAL SYSTEMS

For studying the absorption of iodine solution by plants, dif tial tomographs have been carried out, at energies above and the K-discontinuity of iodine at 33.164 keV. To this purpose, Ray tube with secondary interchangeable targets has been em (Cesareo & Viezzoli, 1983). Secondary targets of Cerium (K=34. and Barium (K=32keV) have been used, and the difference betwe two tomographs has been finally determined, which is only sen to the presence of iodine (Cesareo et al., 1988). A typical is shown in figure 15.

With the same method, the accumulation of Gd-DTPA complex i specific organs of mice has been studied, after intravenous tion. An Am^{241} (200 mCi) source has been employed, which emit keV gamma-rays are selectively attenuated by Gadolinium.

The tomographs of a section of a mouse-kidney is shown in 16.

6. CONCLUSIONS

Main conclusions obtained are:

(1) The calibration curve in linear attenuation coeffic $\mu(cm^{-1})$ versus water content in soil $\theta(cm^3/cm^3)$ at 6Ø ke dicates the viability for water content measurements in science. This confirm previous results of Crestana et (1986).

) The standard deviation from the mean attenuation did not change significantly with the beam width, however, the counting time was adjusted so that equal number of photons contributed to each image. For the images generated with the computerized minitomograph scanner system the better spatial resolution at a pixel width of 1.Ømm was confirmed.

i) The system can be used at all incident energies and with different radiation-sources such as isotopic sources or X-Ray tubes with secondary targets (Cesareo et al., 1988).

) The system is dedicated for soil science research, such as to perform bulk density and water content tomographic analysis.

LEDGEMENTS

RAPA-UAPDIA, Sao Carlos, Brazil and the ICTP Programme for ng and Research in Italian Laboratories, Trieste, Italy for the ial and institutional support. The present work was part of the ements for teh obtention of the PhD degree of Cruvinel, P.E. at iversity of Campinas, S.P., Brazil.

REFERENCES

CESAREO, R.; GIANNINI, M. & Storelli, L. 1982. A miniature X-Ray tomography scanner employing radioisotopic sources. In: INTERNATIONAL CONFERENCE ON APPLICATIONS OF PHYSICS TO MEDICINE AND BIOLOGY, Trieste, Italy, March 30-April 3, 1982. Proceedings...Trieste,ICTP p. 631

CESAREO, R.; VIEZZOLI, G. 1983. Trace elements analysis in biological samples by using XRF spectrometry with secondary radiation. Physics in Medicine & Biology, 28; 1209

CESAREO, R., et al. 1988. Applications of differential tomography to biomedical systems; submitted to Phys. Med.

CRESTANA, S.; CESAREO, R. & MASCARENHAS, S. 1986. Using a computed tomography miniscanner in soil science. Soil Science, 142(1):56-61

CRESTANA, S.; MASCARENHAS, S. & POZZI-MUCELLI, R.S. 1985. Static and dynamic three-dimensional studies of water in soil using computed tomographic scanning. Soil Science, 140(5): 326-32

HAINSWORTH, J.M. & AYLMORES, L.A.G. 1983. The use of computer-assisted tomography to determine spatial distribution of soil water content. Aust. J. Soil Res., 21-435-43

HILLEL, D. 1971. Soil and water: physical principles and process. New York, Academic Press. 365p

PETROVIC, A.M.; SIEBERT, J.E. & RIEKE, P.E. 1982. Soil bulk density analysis in three dimensions by computed tomographic scanning. Soil Sci. Soc. Am. J., 46:445-50

AB, G.O. & FREVERT, R.K. 1985. Elementary soil and water engineering. New York, J. Wiley. 350p

SSON, C.M. & EVANS, R.D. 1952. Gamma-ray absorption coefficients. Rev. Mod. Phys., 24(2): 79-106

CHANDRAN, G.N. & LAKSHMINARAYANAN, A.V. 1971. Three dimensional reconstruction from radiographic and electron micrographic application of convolutions instead of Fourier transforms. Proceedings of the National Academy of Sciences, 68:2236-40

OR, T. & LUPTON, R. 1986. Resolution, artifacts and the design of computed tomography systems. VIII. Tomography. Nuclear Instruments and Methods in Physics Research, A242:603-9

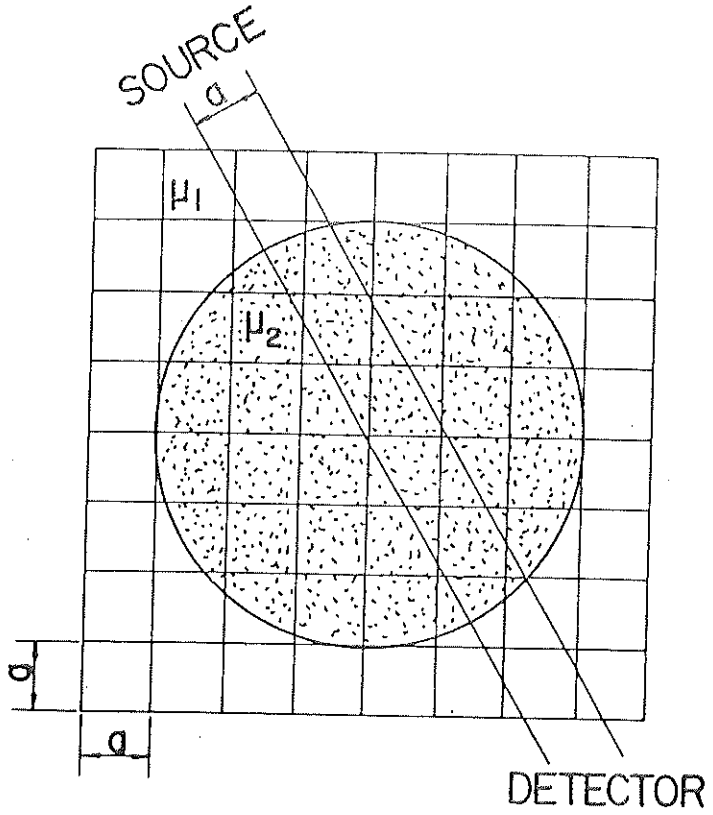

Figure 1 - Scheme of the source-sample-detector configuration.

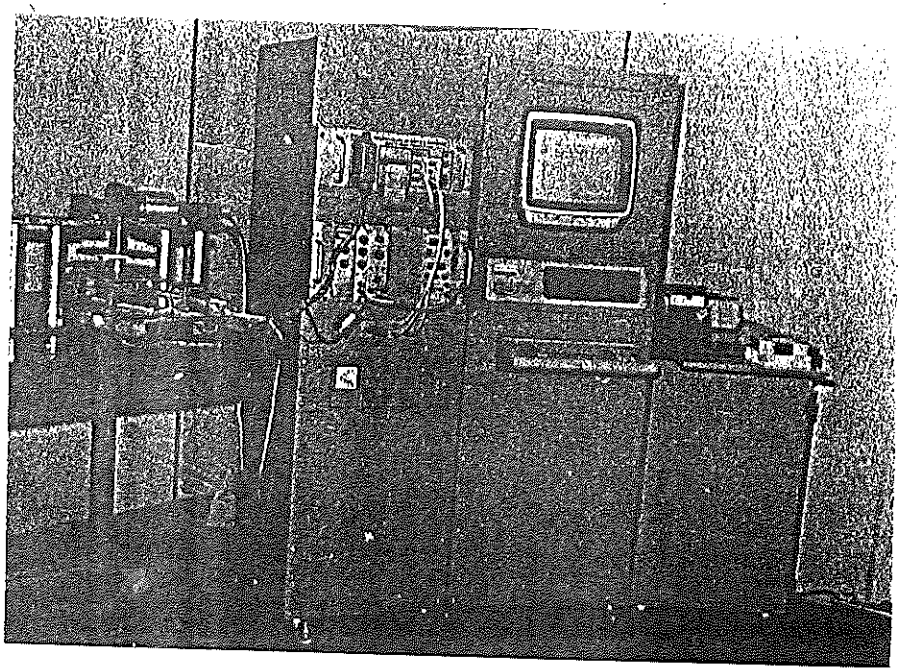

e 2 - Photography of the mini-CT-scanner realized at EMBRAPA (S. Carlos, S.P., Brasil).

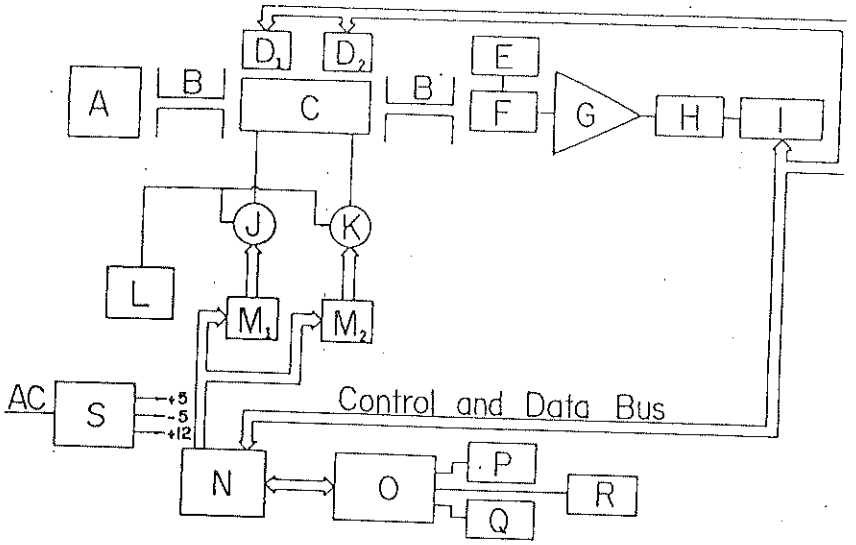

Figure 3 - Block diagram: A = X-ray of gamma-ray source
B = collimator
C = tomographic table
D_1 = control cards for rotation
D_2 = control cards for translation
E = HV power supply
F = detector
G = amplifier
H = single-channel analyzer
I = counter and timer
J = rotation step-motor
K = translation step-motor
L = power supply for step-motors and auxiliar ci
M_1 = rotation control-card
M_2 = translation control-card
N = interface and control
O = microcomputer
P = graphic printer
Q = video-monitor
R = drivers
S = electrical control.

PA 7	PA 6	PA 5	PA 4	PA 3	PA 2	PA 1	PA Ø
$Control_2$	$Clear_T$	$Control_2$	$Clock_T$	$Control_2$	$Clear_R$	$Control_1$	$Clock_R$

Figure 4 - DRA - (PIA-A) .

PB 7	PB6	PB5	PB4	PB3	PB2	PB1	PB Ø
X	X	X	Translation table position	Rotation table position	Test for end count	Start count	Reset counter

Figure 5 - DRB - (PIA-A)

PA 7	PA 6	PA 5	PA 4	PA 3	PA 2	PA 1	PA Ø
X	X	X	X	D_8	D_4	D_2	D_1

Figure 6 - DRA - (PIA-B)

PB 7	PB6	PB5	PB4	PB3	PB2	PB1	PB Ø
X	X	X	X	Digit Advance	TM	PM	Data Transference

Figure 7 - DRB - (PIA-B)

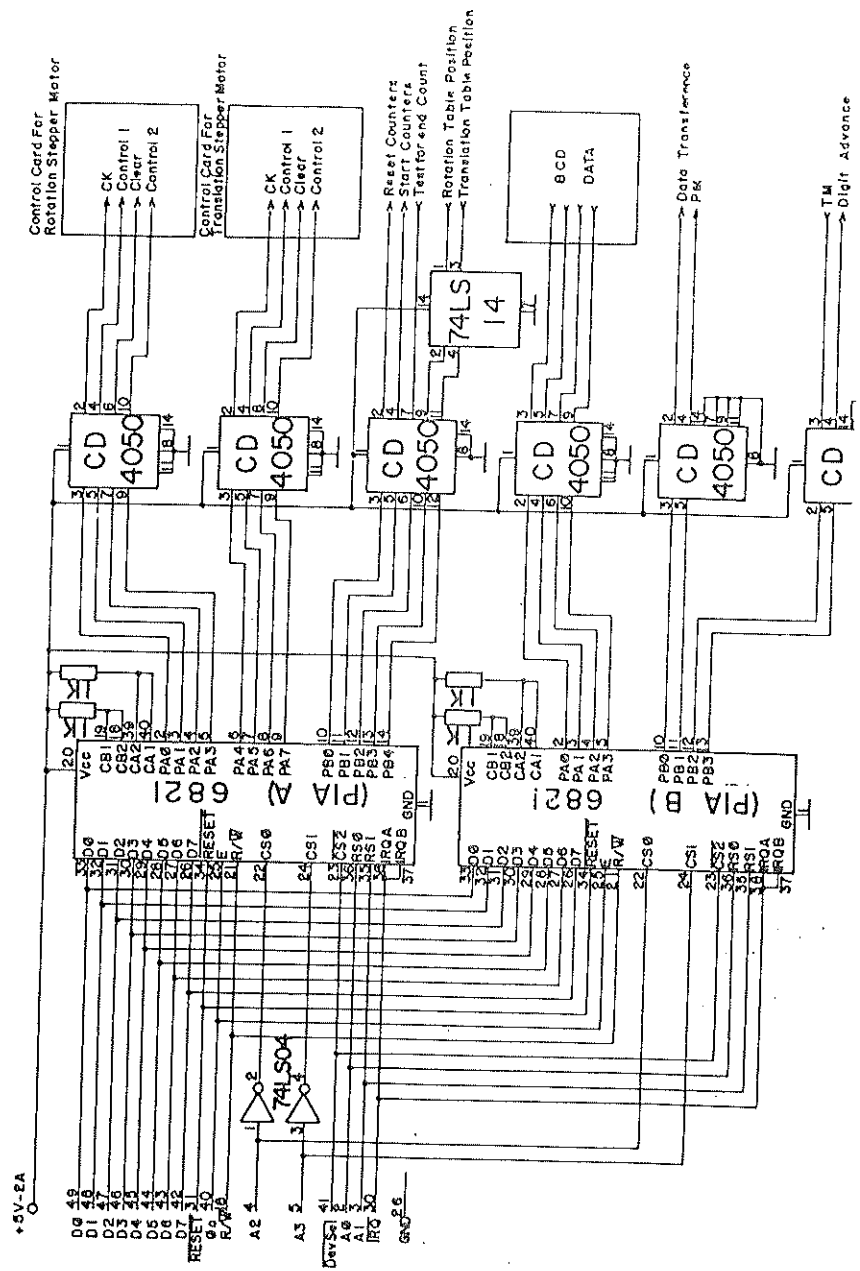

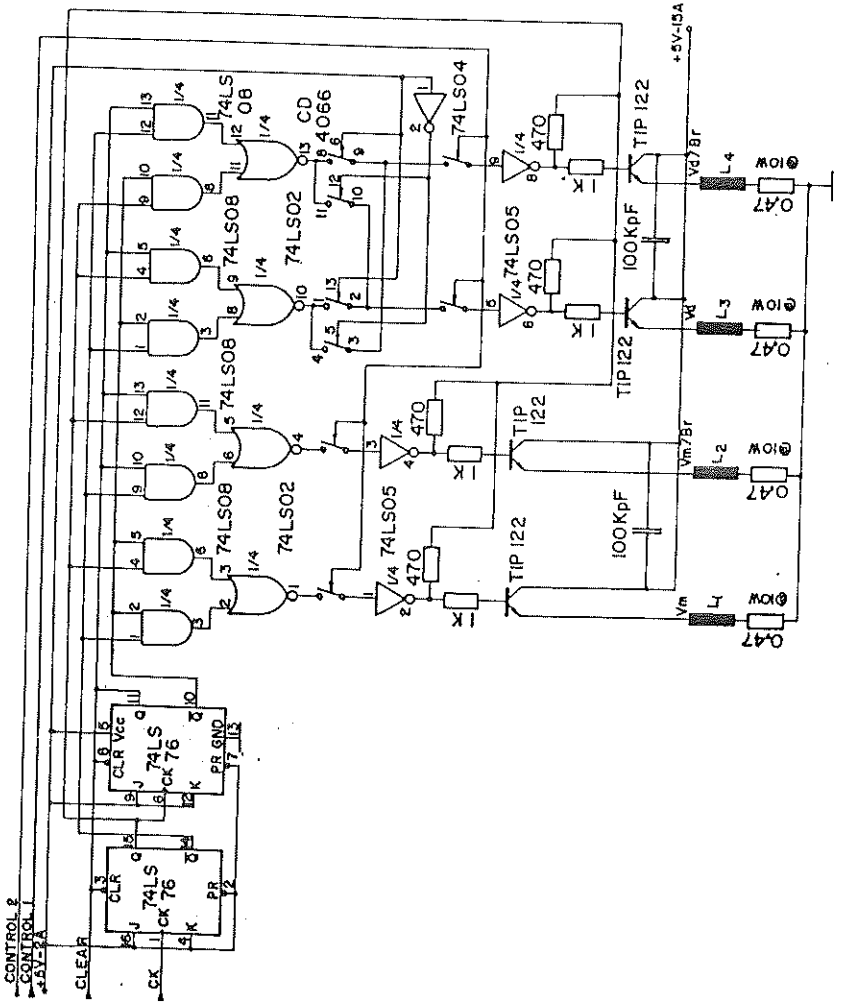

Figure 9 - Schematic diagram for step motors control cards.

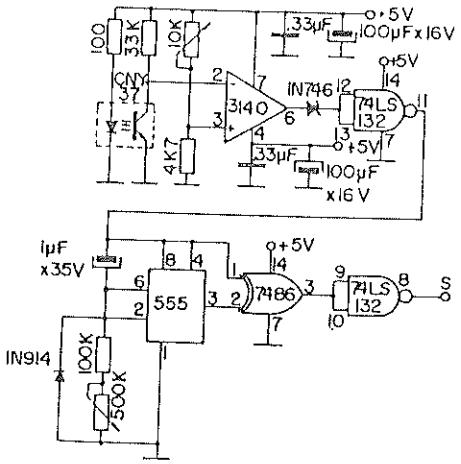

Figure 10 - Schematic diagram for tomographic table position's control cards.

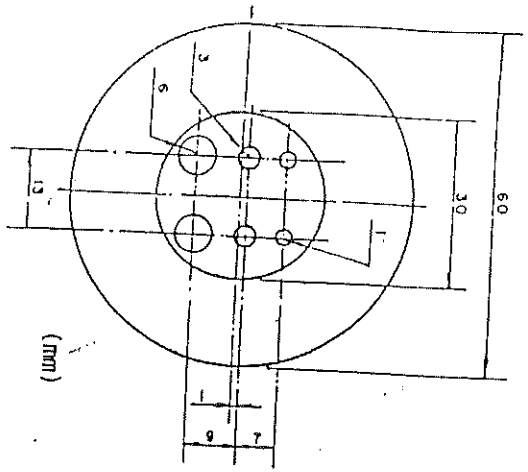

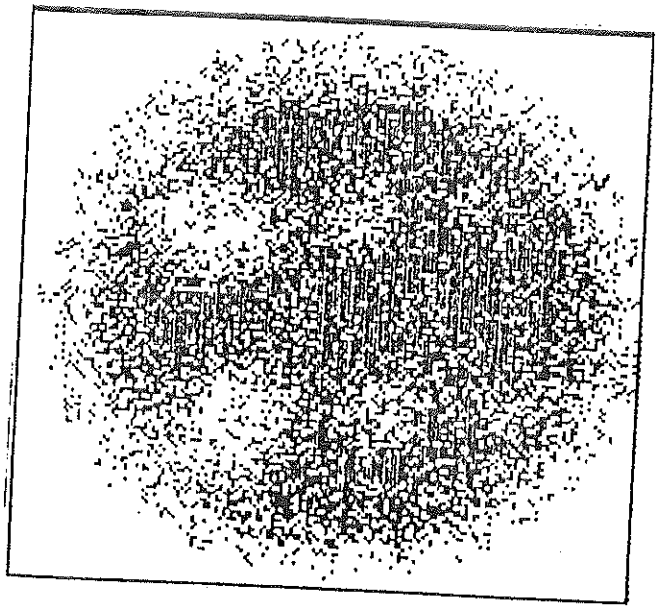

Figure 13 - Test object and image reconstruction on pixel with width of 1.0 mm.

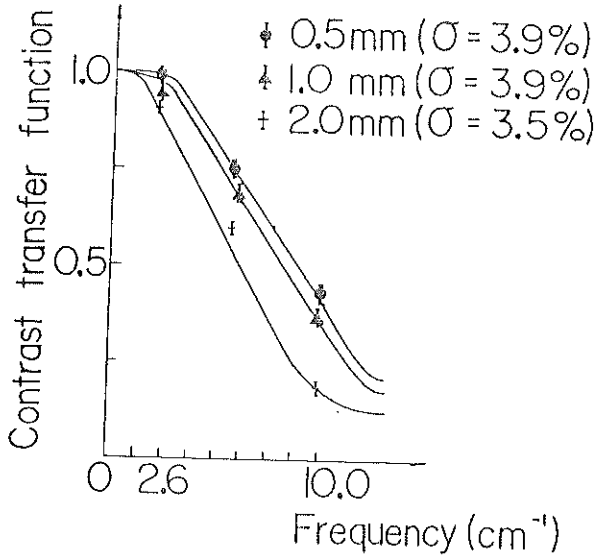

Figure 14 - Contrast transfer function and relative standard deviation for pixel widths of 0.5, 1.0 and 2.0 mm.

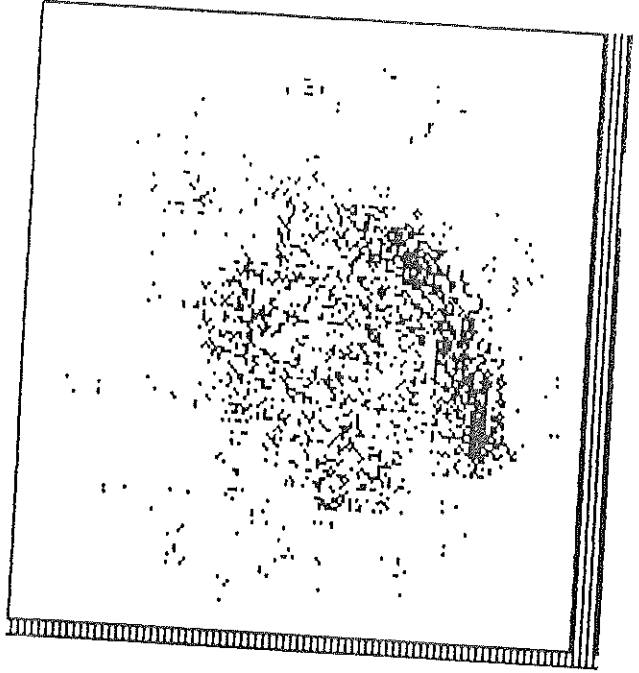

Figure 15 - Differential tomography showing the uptake and selective distribution of Iodine solution in the stem of an "azalea" plant. The maximum value of the attenuation coefficient is 0.416 cm^{-1} and is due to the Iodine-contribution only.

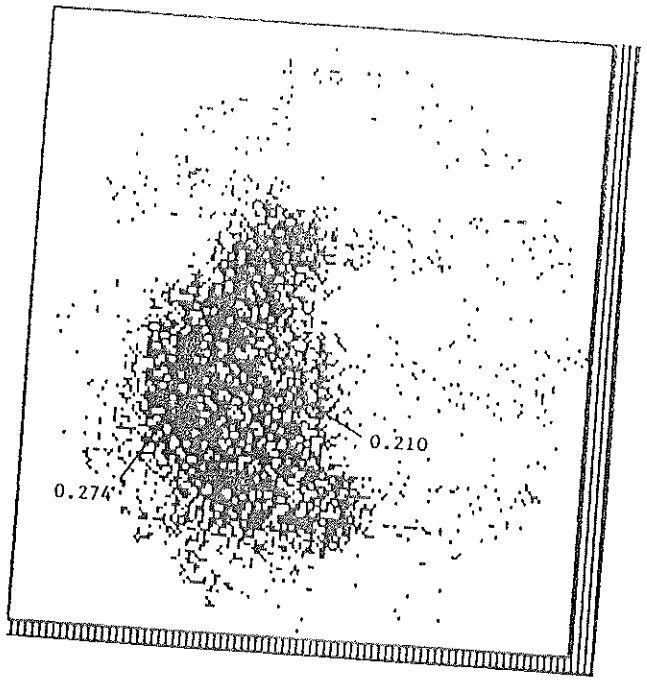

Figure 16 - Tomography of a section of the body of a mouse in which a Gd-DTPA complex was injected. The maximum and minimum values of the attenuation coefficient (0.274 and 0.210) inside the body can be compared with the value (0.210) of the attenuation coefficient of a "non doped" mouse.